Journal of Engineering and Technology Research Vol. 2(7), pp. 118-125, July 2010
Available online at http://www.academicjournals.org/JETR
ISSN 2006-9790 ©2010 Academic Journals

Full Length Research Paper

Strain energy distribution in an auxetic plate with a crack

S. K. Bhullar[1]*, J. L. Wegner[1] and A. Mioduchowski[2]

[1]Department of Mechanical Engineering, University of Victoria, Victoria, B.C. Canada V8W 3P6, Canada.
[2]Department of Mechanical Engineering, University of Alberta, Edmonton, AB, Canada, T6G 2G8, Canada.

Accepted 24 June, 2010

Compared with non-auxetic materials, auxetic materials have special and desirable mechanical properties. For example, if the material has a crack, when it is being pulled apart, it expands and closes up the crack. In other words, this type of material has more crack resistance to fracture. Also, it has high material resistance to shear strain. Shear resistance is particularly important in structural components such as sheets or beams in buildings, cars and aircraft. In the present paper strain energy density, temperature variation, thermal stresses and total stresses in an infinite plate of auxetic material with a line crack, subjected to the mechanical and thermal loading in the context of thermo elastic theory are studied.

Key words: Auxetic behavior, thermal stresses, strain energy function, temperature variation.

INTRODUCTION

Materials with negative Poisson's ratio characterized as auxetic materials have been of significant scientific interest and also have considerable practical applications. A number of potential applications of the auxetic behavior for the design of innovative materials and structural elements or for new processing techniques have been outlined in the engineering literature. The importance of using cork, which is a material with nearly zero Poisson's ratio, for sealing wine bottles, is well known. Another class of applications is based on the sound-absorbing properties of auxetic materials, which make them interesting for both civil and military applications. Furthermore, several authors speculate auxetic behaviour in biomechanics (for example, for the spongy part of the bones), with obvious implications for the efficient design of prostheses. Recently, European patents have proposed annuplastry prostheses that provide plastic repair of a cardiac valve.

LITERATURE REVIEW

A number of potential applications of the auxetic behaviour for the design of innovative materials and structural elements or new processing techniques have been outlined in the engineering literature. Lam et al. (1992) studied the perturbation effects caused by the presence of a crack on thermal stresses, displacements and stress intensity factors in an isotropic linear elastic medium with varying crack surface heat conductivity under uniform heat flow. Minguez (1993) analyzed elastic behavior and some fracture mechanics concepts, such as the geometry factor and the fracture toughness of an infinite plate and a finite plate with a central crack. Shindo et al. (1998) analyzed the scattering of time harmonic flexural waves by a thorough crack in a symmetric piezo-electric laminated plate subjected to electric field loading in the context of dynamic theory of linear piezoelectricity.

The transient thermal conduction problem of a finite plate with multiple insulated cracks and a dynamic problem for two equal rectangular cracks in an infinite elastic plate are studied by Chang and Ma (2001) and Itou (2002) respectively. Coker et al. (2003) presented experimental and numerical results for a dynamic crack growth along the interface of a fiber-reinforced polymer composite-Homalite bimaterial subjected to impact shear loading. A periodic group crack problems in an infinite plate is studied by Chen and Lin, (2005) while Yetmet and Gecit (2005) investigated normal and shearing stress distributions and the stress intensity factors at the edges

*Corresponding author. E-mail: sbhullar@uvic.ca.

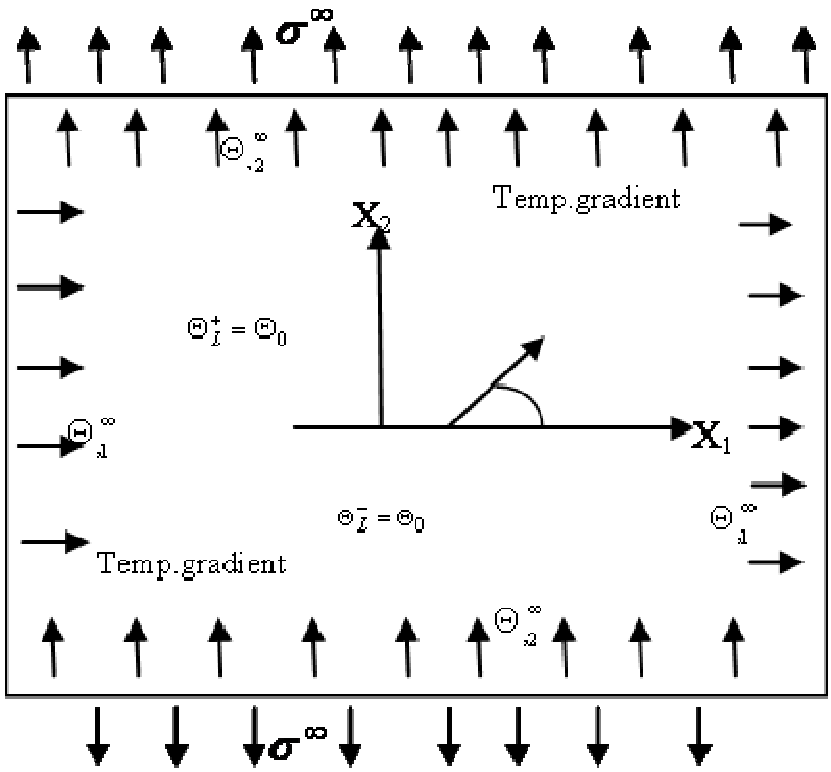

Figure 1. The geometry of the problem.

of the crack and at the corners of the finite strip. Ayatollahi and Aliniaziazi (2006) investigated the effect of the load applied parallel to the crack (or the lateral load) in prestressed square plate containing a center crack. Wu (2006) evaluated stress intensity factor distribution for a surface crack under Mode-I loading conditions. An exact closed-form stress intensity factor solutions have been developed through-thickness cracks in an infinite plate by Lee-Tan et al. (2007) and Feng and Su (2007) obtained solution for the dynamic anti-plane problem for a functionally graded magneto-electro-elastic plate containing an internal or an edge crack parallel to the graded direction. De Matos and Nowell (2008) presented three-dimensional finite element analyses of a plate with a central crack to investigate the effect of corner point singularities. Bogdan (2009) studied a problem of a thin plate made of a piezoelectric ceramic material containing a crack perpendicular to its surfaces. Also, Guo et al. (2009) obtained an analytical solution for an eccentric crack loaded by shear forces in a finite width plate using crack line analysis method.

There are two basic ways in which a volume element can store energy, by dialation which is associated with change in volume and distortion which is associated with the change in shape. When an element of the material exceeds a certain energy threshold fracture could occur. Auxetic materials possess more crack resistance to fracture. Thus, if this type of material has a crack, when it is being pulled apart, it expands and closes up the crack. In this paper strain energy density, temperature variation, thermal stresses and total stresses in an infinite plate of auxetic material with a line crack, subjected to the mechanical and thermal loading in the context of thermo elastic theory is studied.

MODEL AND METHODS

An analytical solution is obtained under the boundary condition that the constant temperature is retained on the crack surfaces while the remote uniform heat flow is applied. For this purpose an infinite plate with a central crack of length $2a$, is considered and a uniform heat flow and the uniform tensile stress σ^{∞} is applied at infinity. There is an angle between the directions of heat flow and crack line. The heat flow vector can be resolved into two parts, respectively, along two co-ordinate axis. Two temperature gradient components along two co-ordinate axis at infinity are denoted by $\Theta_{,1}^{\infty}$ and $\Theta_{,2}^{\infty}$ and the heat flow is proportional to the negative temperature gradient. The geometry of the problem is shown in Figure 1.

In this case thermal loading only induces the model stress intensity factor. The heat flow along the vertical

direction has no influence on the thermal stress intensity factor. The problem is typical model crack problem. There is no heat source in the plate, thus governing differential equation in this case is:

$$\nabla^2\Theta = 0 \tag{1}$$

Assume that the temperature on the upper and lower surfaces of the crack remains constant

$$\Theta_L^+ = \Theta_L^- = \Theta_0, \text{ on L.} \tag{2}$$

The symbol "L" denotes the crack and "+" and "-" stand for, respectively, the upper and lower crack surfaces. Θ_0 is the constant temperature on the upper and lower crack surfaces. Further, the full field temperature solution is given by Tang (2009):

$$\Theta = \frac{1}{2}\Theta_{,1}^{\infty}\left(\sqrt{z^2-a^2}+\sqrt{\bar{z}^2-a^2}\right)-\frac{\iota}{2}\Theta_{,2}^{\infty}(z-\bar{z})+\Theta_0 \tag{3}$$

and the asymptotic solution of the temperature near the crack tip is expressed as

$$\Theta = \frac{1}{2}\Theta_{,1}^{\infty}\sqrt{2ar_1}\cos\frac{\theta}{2}+\Theta_{,2}^{\infty}r_1\sin\theta+\Theta_0 \tag{4}$$

Where, R is the distance from the crack tip, z and $\bar{z}$ are complex conjugate.

Also, the asymptotic solution of the thermal stresses and the expression of the stress intensity factor are:

$$\sigma_{11}^{\Theta} = \frac{K_1^{\Theta}}{\sqrt{2\pi r_1}}\cos\frac{\theta}{2}\left(1-\sin\frac{\theta}{2}Sin\frac{3\theta}{2}\right) \tag{5}$$

$$\sigma_{22}^{\Theta} = \frac{K_1^{\Theta}}{\sqrt{2\pi r_1}}\cos\frac{\theta}{2}\left(1+\sin\frac{\theta}{2}\sin\frac{3\theta}{2}\right) \tag{6}$$

$$\sigma_{12}^{\Theta} = \frac{K_1^{\Theta}}{\sqrt{2\pi r_1}}\sin\frac{\theta}{2}\cos\frac{\theta}{2}\cos\frac{3\theta}{2} \tag{7}$$

$$K_1^{\Theta} = \frac{\alpha E a\,\Theta_{,1}^{\infty}}{\kappa+1}\sqrt{\pi a}, \quad \kappa = 3-4\nu, \tag{8}$$

$$K_2^{\Theta} = 0 \tag{9}$$

Where, α, E, ν, K_1^{Θ} and K_2^{Θ} are linear expansion coefficient, Young's modulus, Poisson's ratio and stress intensity factor, respectively. The superscript Θ denotes the thermal effect. As this problem is a typical crack problem of mode I, the stress intensity factor is only related to the heat flow along x_1- direction. The heat flow along x_2- direction does not produce thermal stresses. Further under the combination of thermal and mechanical loading, the asymptotic solution of total stress field in the vicinity of crack tip is:

$$\sigma_{11} = \frac{K_1}{\sqrt{2\pi r_1}}\cos\frac{\theta}{2}\left(1-\sin\frac{\theta}{2}\sin\frac{3\theta}{2}\right) \tag{10}$$

$$\sigma_{22} = \frac{K_1}{\sqrt{2\pi r_1}}\cos\frac{\theta}{2}\left(1+\sin\frac{\theta}{2}Sin\frac{3\theta}{2}\right) \tag{11}$$

$$\sigma_{12} = \frac{K_1}{\sqrt{2\pi r_1}}\sin\frac{\theta}{2}\cos\frac{\theta}{2}Cos\frac{3\theta}{2} \tag{12}$$

$$\sigma_{33} = \nu(\sigma_{11}+\sigma_{22})-\alpha E\Theta, \quad \sigma_{13}=\sigma_{23}=0 \tag{13}$$

Where, K_1 total stress intensity factor is the sum of the mechanical and thermal parts, r_1 and θ are the polar coordinates measured from the crack tip as shown in Figure 1. The term $\alpha E\theta$ in equation (13) is nonsingular because the temperature field is nonsingular at the crack tip in view of equations (3)-(4). It can be omitted.

$$K_1 = K_1^{\sigma}+K_1^{\Theta}, \quad K_1^{\sigma} = \sigma^{\infty}+\sqrt{\pi a}, \quad K_1^{\Theta} = \frac{\alpha E a\,\Theta_{,1}^{\infty}}{\kappa+1}\sqrt{\pi a}$$

$$K = \left(\sigma^{\infty}+\frac{\alpha E a\,\Theta_{,1}^{\infty}}{\kappa+1}\right)\sqrt{\pi a}\,. \tag{14}$$

Equation (14) indicate that the temperature gradient $\Theta_{,1}^{\infty}$ can be regarded as an equivalently applied stress at infinity denoted by σ_{Θ}^{∞} which is written as

$$\sigma_{\Theta}^{\infty} = \frac{\alpha E a\,\Theta_{,1}^{\infty}}{\kappa+1} \tag{15}$$

Therefore, the total applied stress at infinity is equal to

$$\sigma = \sigma^{\infty}+\sigma_{\Theta}^{\infty} \tag{16}$$

Where, σ^{∞} is the mechanical part and σ_{Θ}^{∞} is the thermal part. Bodies having large volume to surface ratio dissipate more energy by dilatation in contrast to distortion. The dominance of dilatation tends to exhibit brittle behavior. As the volume to surface ratio is de-creased, energy dissipation via distortion would overtake that of dilatation and a unit volume of the same material become more ductile. The ductile-brittle transition depends on the material microstructure, specimen shape and size, temperature and rate of deformation.

Regardless of nonlinearity, the proportion of energy

Table 1. Material properties.

Material parameter	Copper foam	Steel alloy
E, Young's modulus	30 (GPa)	200GPa
Linear thermal expansion α	0.55×10-6 (1/0C)	12.94 × 10-6 (1/0C)
Poisson's ratio	-0.7	0.33

expanded by dilatation and distortion can be assessed from the stationary values of the energy density function. The strain energy density criterion can be applied to predict the crack initiation and extension in isotropic materials. Making use of the stress and strain components σ_{ij} and ε_{ij} the strain energy density given by Carloni and Nobile, 2008:

$$\frac{dW}{dV} = \int_0^{\varepsilon_{ij}} \sigma_{ij} d\varepsilon_{ij}$$

Further, for linear elasticity the above equation is expressed as

$$\frac{dW}{dV} = \frac{1}{2}\sigma_{ij}\varepsilon_{ij} \quad (17)$$

Constitutive relation of linear thermoelasticity is

$$\varepsilon_{ij} = \frac{1+\nu}{E}\sigma_{ij} - \frac{\nu}{E}\sigma_{kk}\delta_{ij} + \alpha\Theta\delta_{ij} \quad (18)$$

Where, Θ stands for the temperature to the reference temperature. The expressions obtained (see Appendix I) for strain energy density, dialation part and distortional part of strain energy density are as follows:

$$\frac{dW}{dV} = \frac{(1+\nu)(1+\cos\theta)(3-4\nu-\cos\theta)}{8\pi E r_1} K_1^2 \quad (19)$$

$$\left(\frac{dW}{dV}\right)_v = \frac{(1-2\nu)(1+\nu)^2(1+\cos\theta)}{6\pi E r_1} K_1^2 \quad (20)$$

$$\left(\frac{dW}{dV}\right)_d = \frac{(1+\nu)(1+\cos\theta)\left[2(1-2\nu)^2+3(1-\cos\theta)\right]}{24\pi E r_1} K_1^2 \quad (21)$$

In the linear elastic fracture mechanics theory, the strain energy density factor S is defined as $\frac{dW}{dV} = \frac{S}{r_1}$

And the strain energy density factor S is in form of (Appendix I)

$$S = A_{11}\left(\sigma^{\infty}\right)^2 + 2A_{12}\sigma^{\infty}\Theta_{,1}^{\infty} + A_{22}\left(\Theta_{,1}^{\infty}\right)^2 \quad (22)$$

$$A_{11} = \frac{(1+\nu)(1+\cos\theta)(3-4\nu-\cos\theta)a}{8E} \quad (23)$$

$$A_{12} = \frac{(1+\nu)(1+\cos\theta)(3-4\nu-\cos\theta)\alpha a^2}{32(1-\nu)} \quad (24)$$

$$A_{22} = \frac{(1+\nu)(1+\cos\theta)(3-4\nu-\cos\theta)\alpha^2 E a^3}{32(1-\nu)} \quad (25)$$

RESULTS AND CONCLUDING REMARKS

The problem of an infinite plate with a central crack subjected to the remote uniform heat flow along any direction has been solved by the complex function method. To study the auxetic behavior of an infinite plate with a central crack of length 2a the results for temperature variation, stress field, strain energy distribution-the dilatational and distortional part of strain energy function and strain energy factor are obtained and are shown graphically. The copper foam and steel alloy are the material chosen to perform the numerical calculations and the material parameters are given in Table 1. The temperature gradient components along two co-ordinate axis at infinite are taken as $\Theta_{,2}^{\infty}$ =100K/m= $\Theta_{,2}^{\infty}$, constant temperature $\Theta_o = 100K$, $a = 10mm$ and the uniform tensile stress applied at infinite, σ^{∞} =10MPa . The temperature variation versus angle θ (radians) in the crack region due to non-dimensional distance, $r = \frac{r_1}{a}$, is illustrated in Figure 2. By the combination of mechanical and thermal loading the total stress field in the neighborhood of crack tip is shown in Figures 3 to 6 and symmetrical behavior is observed. It is noticed that for the stress component σ_{33} in Figure 6, the pattern of curves is the same as in the case of temperature distribution but in opposite direction.

The contours of strain energy density, distortional part and dilatational part of strain energy density are shown in

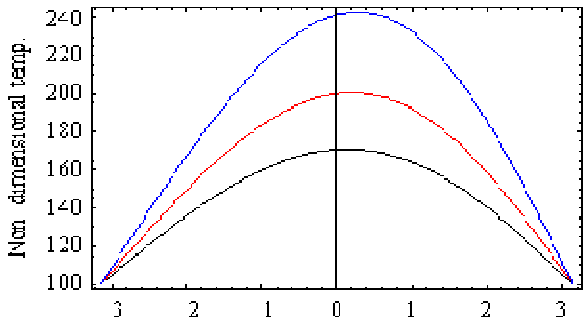

r = 0.25

r = 0.05

r = 0.1

Figure 2. Temperature variation near the crack due to normalized distance.

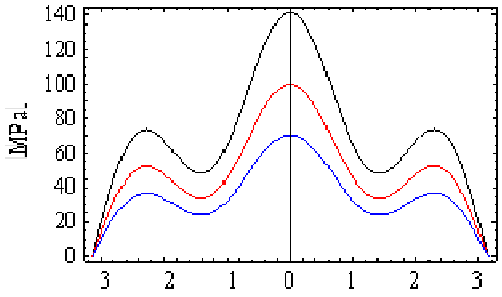

r = 0.25

r = 0.5

r = 0.1

Figure 3. Stress component σ_{11}, near crack tip.

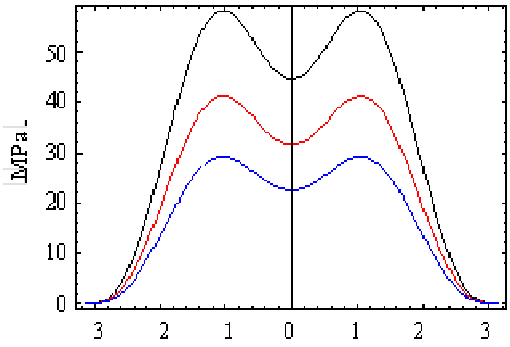

r= 0.25

r=0.5

r=0.1

Figure 4. Stress component σ_{22}, near crack tip.

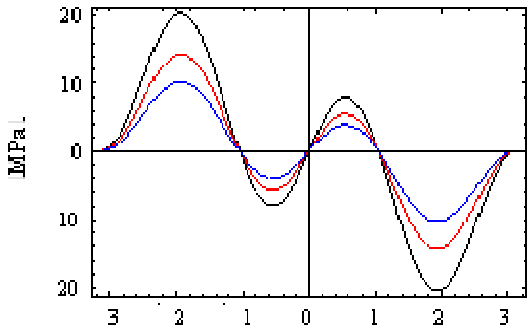

r= 0.25

r = 0.5

r = 0.1

Figure 5. Stress component σ_{12}, near crack tip.

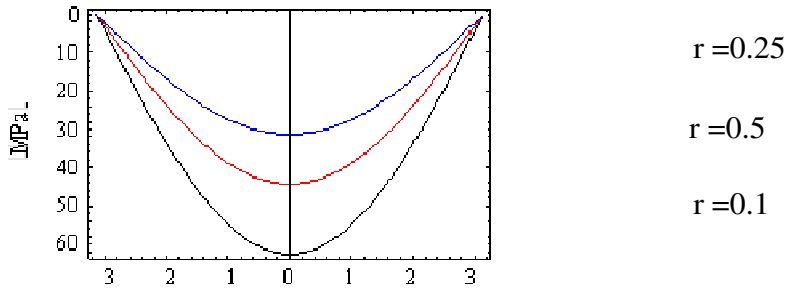

Figure 6. Stress component σ_{33}, near crack tip.

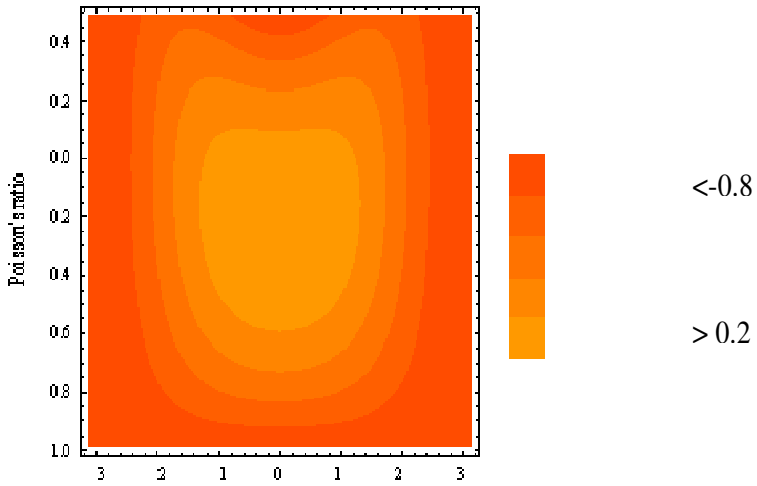

Figure 7a. Strain energy density crack tip.

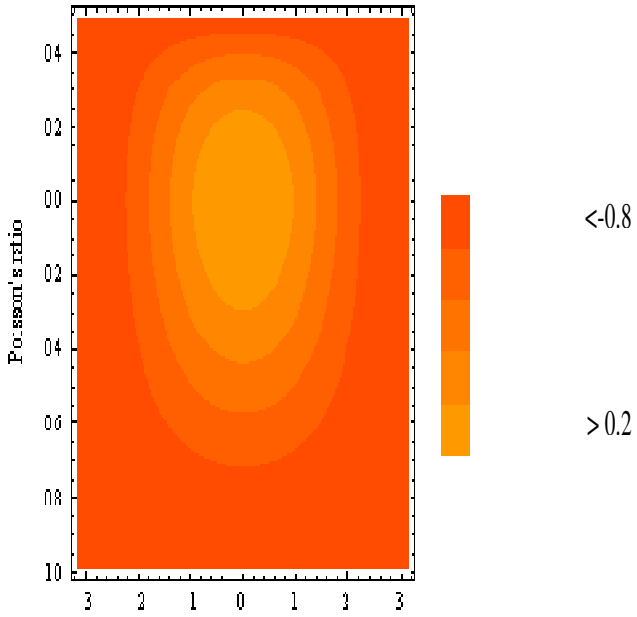

Figure 7b. Strain energy density (dilatational) near crack tip.

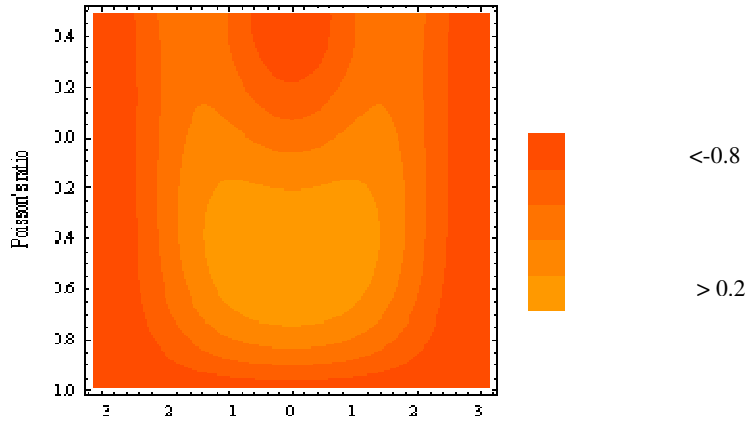

Figure 7c. Strain energy density (distortional) near crack tip.

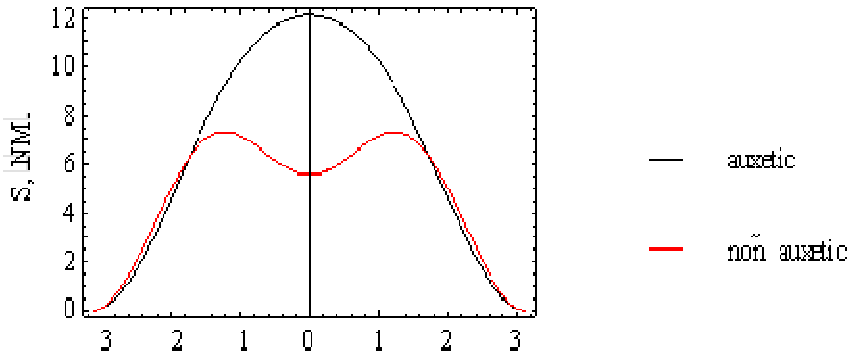

Figure 8. Comparison of strain energy density factor, S.

Figure 7a-c. It is clear, the contours of $\left(\frac{dW}{dV}\right)$, $\left(\frac{dW}{dV}\right)_d$ and $\left(\frac{dW}{dV}\right)_v$ are not affected by the thermal effect.

The comparison of strain energy factors *S* for non-auxetic and auxetic material is shown in Figure 8. It is observed that maximum value of *S* occurs at angle, $\theta = 0$ in the case of auxetic material and the local minimum value of *S* in the case of non-auxetic material. It is clear when compared with non-auxetic materials that auxetic materials have almost twice crack resistance to fracture.

REFERENCE

Ayatollahi MR, Aliniaziazi A (2006). Effects of lateral load on warm pre-stressing in a center crack plate, J. Mater. Sci. Eng., 441: 170-175.
Bogdan R (2009). The transient thermo-electro-elastic fields in a piezoelectric plate with a crack, Int. J. Pressure Vessels Piping 86: 384-394.
Carloni C, Nobile L (2008). Crack initiation behavior of orthotropic solids as predicted by the strain energy density theory, Theoret. Appl. Fract. Mech. 38: 109-119.
Chang C-Yi, Ma C-C (2001). Transient thermal conduction analysis of a rectangular plate with multiple insulated cracks by the alternating method, Int. J. Heat Mass Transfer, 44: 2423-2437.
Chen YZ, Lin XY (2005). Periodic group crack problems in an infinite plate, Int. J. Solids Struct., 42: 2837-2850.
Coker D, Rosakis AJ, Needleman A (2003). Dynamic crack growth along a polymer composite–Homalite interface, J. Mech. Phys. Solids, 51: 425-460.
De Matos PFP, Nowell D (2008). The influence of the Poisson's ratio and corner point singularities in three-dimensional plasticity-induced fatigue crack closure a numerical study, Int. J. Fatigue, 30: 1930-1943.
Feng W, Su R (2007). Dynamic fracture behaviors of cracks in a functionally graded magneto-electro-elastic plate, Eur. J. Mech. - A/Solids, 26: 363-379.
Guo C, Zhou XP, Zhang YX, Yang HQ, Li XH (2009). Elastic–plastic near field solution of an eccentric crack under shear in a finite width plate, Theoret. Appl. Fract. Mech., 51: 174-180.
Itou S (2002). Dynamic stress intensity factors around two rectangular cracks in an infinite elastic plate under impact load, Mech. Res. Commun., 29: 225-234.
Lam KY, Tay TE, Yuan WG (1992). Stress intensity factors of cracks in finite plates subjected to thermal loads, J. Eng. Fract. Mech., 43: 641-650.
Lee-Tan JM, Fitzpatrick ME, Edwards L (2007). Stress intensity factors

for through-thickness cracks in a wide plate: Derivation and application to arbitrary weld residual stress fields, J. Eng. Fract. Mech., 74: 2030-2054.
Minguez JM (1993). Study of elastic behaviour of plates containing cracks by finite element analysis, J. Comp. Struct., 47: 917-925.
Yetmet M, Gecit MR (2005). Finite strip with a central crack under tension, Int. J. Eng. Sci., 43: 472-493.
Shindo Y, Domon W, Narita F (1998). Dynamic bending of a symmetric piezoelectric laminated plate with a through crack, Theoret. Appl. Fract. Mech., 28: 175-182.
Tang XS (2009). Mechanical thermal stress intensification for mode I crack tip, Theoret. Appl. Fract. Mech., 50: 92-104.
Wu Z (2006). The shape of a surface crack in a plate based on a given stress intensity factor distribution, Int. J. Pressure Vessels Piping, 83: 168-180.

Appendix 1

By making use of equations (17) - (18) we have obtained following equation:

$$\frac{dW}{dV} = \frac{1+\nu}{2E}\left(\sigma_{ij}\sigma_{ij} - \frac{\nu}{1+\nu}\sigma_{kk}^2\right) = \frac{1+\nu}{2E}\left[\sigma_{11}^2+\sigma_{22}^2+\sigma_{33}^2 - \frac{\nu}{1+\nu}(\sigma_{11}+\sigma_{22}+\sigma_{33})^2 + 2\sigma_{12}^2\right] \quad (1)$$

Upon using equation (13), above equation takes the form for plane strain

$$\frac{dW}{dV} = \frac{1+\nu}{2E}\left[\sigma_{11}^2+\sigma_{22}^2 - \nu(\sigma_{11}+\sigma_{22})^2 + 2\sigma_{12}^2\right] \quad (2)$$

Equation (1) can also written as

$$\frac{dW}{dV} = \frac{3}{2}\sigma_m\varepsilon_m - \frac{1}{2}\alpha\Theta\sigma_{kk} + \frac{1}{2}s_{ij}e_{ij}\left[\sigma_{11}^2+\sigma_{22}^2 - \nu(\sigma_{11}+\sigma_{22})^2 + 2\sigma_{12}^2\right] \quad (3)$$

Where, $\sigma_m = \frac{\sigma_{kk}}{3}$ and $\varepsilon_m = \frac{\varepsilon_{kk}}{3}$ are hydrostatic stress and strain; s_{ij} and ε_{ij} are deviatoric stress and strain. The dilatational part and distortional part of strain energy density are:

$$\left(\frac{dW}{dV}\right)_v = \frac{3}{2}\sigma_m\varepsilon_m - \frac{1}{2}\alpha\Theta\sigma_{kk} \quad (4)$$

$$\left(\frac{dW}{dV}\right)_{dv} = \frac{1}{2}s_{ij}e_{ij} \quad (5)$$

By application of equation (18) in equations (4)-(5) we get:

$$\left(\frac{dW}{dV}\right)_v = \frac{1-2\nu}{6E}(\sigma_{11}+\sigma_{22}+\sigma_{33})^2 = \frac{(1-2\nu)(1+\nu)^2}{6E}(\sigma_{11}+\sigma_{22})^2 \quad (6)$$

$$\left(\frac{dW}{dV}\right)_d = \frac{1+\nu}{6E}\left[(\sigma_{11}-\sigma_{22})^2+(\sigma_{22}-\sigma_{33})^2+(\sigma_{33}-\sigma_{11})^2+6\sigma_{12}^2\right] = \frac{1+\nu}{3E}\left[\sigma_{11}^2+\sigma_{22}^2-\sigma_{11}\sigma_{22}-\nu(1-\nu)(\sigma_{11}-\sigma_{22})^2+3\sigma_{12}^2\right] \quad (7)$$